Behaviour of Reinforced Concrete Walls with Different Opening Locations: Experiment and FEM Analysis

R. Taleb, H. Bechtoula
National Center for Applied Research on Earthquake Engineering (CGS), Algeria

M. Sakashita, S. Kono
Department of Architecture and Architectural Engineering, Kyoto University, Japan

N. Bourahla
Department of Civil Engineering, Saad Dahleb University, Blida, Algeria

SUMMARY:
The aim of this paper is, firstly, to present the experimental results of three reinforced concrete structural walls tested under lateral reversed cyclic loading, two walls with different opening locations and one without opening. The specimens were scaled to 40% single span three storied reinforced concrete structural wall. The main purposes of the experimental tests were to evaluate their behaviour and to identify the influence of opening locations on the cracks distribution and the shear strength. Secondly, to estimate the shear strength of the tested specimens by combining the shear strength of structural wall without openings and the reduction factor due to openings. The comparison between the experimental results and the analytical results showed that the shear strength was different depending on the loading direction and the opening locations. A two-dimensional FEM analytical model was constructed in order to predict the behaviour of the tested walls. A good agreement was found between the test and the prediction in terms of lateral load-drift angle relations and damage distribution.

Keywords: multi-story RC walls; static test; shear behaviour; nonlinear FEM analysis.

1. INTRODUCTION

Reinforced concrete structural walls are one of the main earthquake-resisting components for RC high-rise and mid-rise buildings. Experience from past earthquakes has shown that buildings with well-designed structural walls can significantly reduce life and economic losses (AIJ, 1998 ; Bechtoula and Oussalem, 2005). For functional reasons, the structural walls may have openings like windows, doors and duct spaces. The opening sizes, locations and shapes of openings affect their seismic performance by reducing the stiffness and the strength of the structural wall.

During the past several decades, numerous experimental studies have been conducted on the behaviour of RC structural walls with and without openings (Ono, 1995; Lopes, 2001, Sakurai *et al.*, 2008, Warashina *et al.*, 2008, Kabeyasawa *et al.*, 2009, Brun *et al.*, 2011). However, the case of large and eccentric openings was not deeply investigated in the past. More experimental data are needed to clarify the shear behaviour of structural walls with eccentric openings under cyclic loading.
In such cases, finite element studies may be the only alternative to understand their behaviour. Nowadays, and due to availability of powerful computers, numerical modelling approaches are able to provide an accurate alternative to the experimental investigations of reinforced concrete structural walls (Maekawa *et al.*, 2003; Kim and Lee, 2003; Balkaya and Kalkan, 2004, Thomson *et al.*, 2009; Guan *et al.*, 2010).

In the current design practice of AIJ standard (AIJ, 2010), the shear strength of a structural wall with opening is estimated by applying a strength reduction factor on the strength of the structural wall without opening. The applicability of this approach is limited for opening ratio less then 0.4. The opening ratio, η, expresses the size of the opening and it is given by:

$$\eta = \max\left\{\sqrt{\frac{h_0 \cdot l_0}{h \cdot l}}, \frac{l_0}{l}\right\} \quad (1)$$

Where, l is the center to center spacing between two side columns, h is the center to center spacing between the upper and lower beams and l_0 and h_0 are the length and height of the opening, respectively, as shown in Figure 1. As it can be seen from Eq. (1), the reduction factor is independent from the opening location.

2. EXPERIMENTAL PROGRAM

2.1. Test specimens

Three RC wall specimens were constructed and tested at Kyoto University. The specimens were three-storied and 40% scaled models. As shown in Figure 2, specimen N1 was without openings, specimens L1 was with eccentric openings and L3 specimen with centric openings, both with opening ratio of 0.46. The main test variables were the opening location. The main purposes of the experimental tests were to evaluate the shear behavior and to clarify the influence of large opening location on the cracks distribution and the shear strength of structural walls under horizontal reversed cyclic loading. The specimens were 4150 mm height and 2800 mm wide. To provide a fixed base at the bottom, a RC foundation beam with 600 mm wide by 400 mm thick and 3600 mm in length was built integrally with the body of the structural walls and post-tensioned to the reaction floor prior to testing. A hydraulic actuator was attached to the specimen at mid-span of the loading beam to apply the horizontal reversed cyclic loading. The third story was provided for releasing the confinement caused by the stiff loading beam at the top. The structural walls were tested in a lateral reverse cyclic manner until their maximum performances. All the specimens were designed to fail in shear and not in flexure.

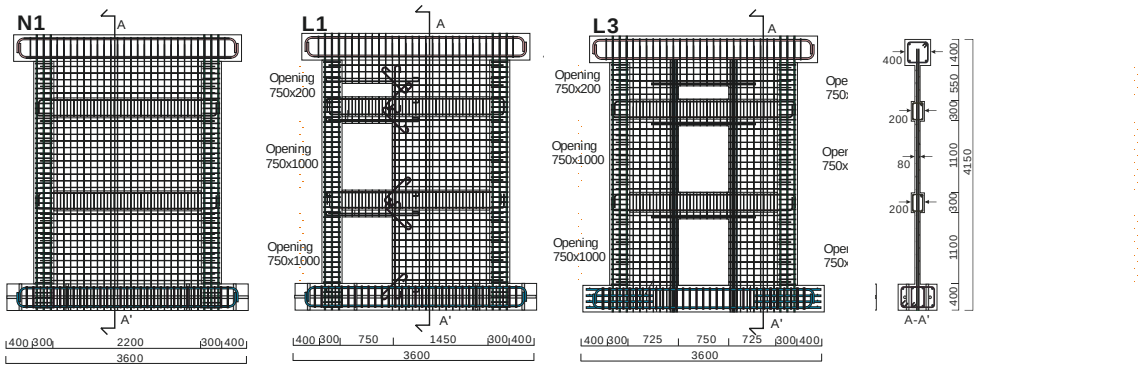

Figure 1. Specimen configurations and reinforcing bars arrangement.

2.2. Material properties

Table 1 shows the cross section dimensions and the reinforcement arrangement. Table 2 shows the reinforcing bars around the openings as well as the opening ratios. Material properties of concrete and reinforcement adopted for the specimens are listed in Tables 3 and 4, respectively.

Table 1. Cross section dimension and reinforcement arrangement

Element	Dimension (mm)	Main bar	Stirrup
Column	300×300	8-D19	2-D6@100
Beam	200×300	2-D13	2-φ10@75
Wall	Thickness 80	Vertical: D6@100	Horizontal: D6@100
Loading beam	400×400	4-D25	2-D10@100
Foundation beam	400×600	8-D25	4-D10@100

Table 2. Reinforcing bars around opening

Specimen	Opening ratio	Vertical reinforcing	Horizontal reinforcing	Diagonal reinforcing
L1	0.46	1-D16	2-D13	1-D16
L3	0.46	4-D13	4-D10	-

Table 3. Concrete material properties

Specimen	Compressive strength (MPa)	Tensile strength (MPa)	Young's modulus (GPa)
N1	25.9	2.3	21.0
L1	28.9	2.5	26.0
L3	32.7	2.9	23.3

Table 4. Reinforcements properties

Nominal diameter	Yield strength (MPa)	Maximum strength (MPa)	Young's modulus (GPa)
D6	425	538	204
D10	352	496	186
D13	362	529	188
D19	411	605	189
D25	387	541	194
φ10	1033	1221	204

2.3. Experimental setup and testing procedure

Figure 2 shows the details of loading system and the loading history, respectively. The lateral load, *Q*, was applied statically to the loading beam by two 2 MN hydraulic jacks. Cyclic reversed horizontal loads were statically applied to the specimens in both positive and negative directions. During the cyclic horizontal loading, vertical axial loads were applied to columns by two 1 MN hydraulic jacks assuming that the specimens are representing the lower three stories of a typical six stories RC building.

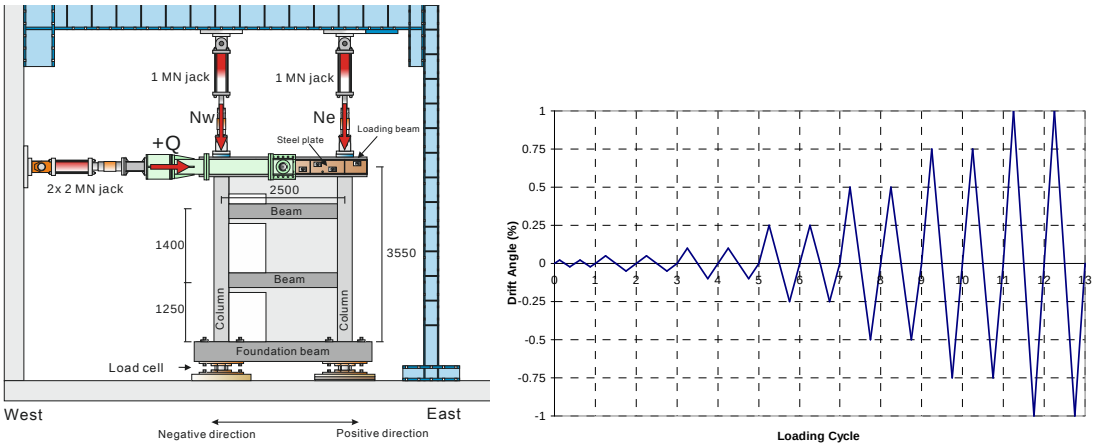

(a) (b)

Figure 2. (a) Experimental setup, loading system and (b) loading history

The vertical axial load levels were determined in accordance with the assumed long-term axial loads for a six-story wall with three spans. The two vertical hydraulic jacks were adjusted to apply two vertical forces, *Nw* and *Ne*, that vary as a function of the applied lateral load, *Q*, in order to keep the shear span ratio (*M/Ql*) equal to 1.0. This will insure that the shear damages in the wall will precede the flexural yielding of the wall. The influence of the axial load level on the shear capacity of each wall was insignificant since the side columns were not damaged until the end of the tests. Loading was

mainly controlled by measured displacement in terms of the story drift angle. The same loading history was used to test all specimens. The loading history was divided into two parts: The first cycle of loading was performed up to 200 kN, after that, two cycles of repeated loading were applied for each drift angle, *R*, of ±0.05, ±0.1, ±0.25, ±0.5, ±0.75, ±1.00 and ±1.5%.

3. INTERPRETATION OF EXPERIMENTAL RESULTS

3.1. Damages and crack pattern

Figures 3(b) to 5(b) show the observed damages at the end of the tests on specimen N1, L1 and L3, respectively. For all specimens, the cracking started with the apparition of diagonal cracks in the wall panels at 0.05% drift angle. Flexural cracks in the tensile side column were also observed. As the applied drift angle increased, the number of shear cracks increased in the wall panels and showed a downward trend illustrating the stress transfer path. For specimens with opening, the formation of a shear transfer truss mechanism was prevented, and the shear stress trended to concentrate at the bottom corner of the openings. When the drift angle increased from 0.5% to 0.75%, the lateral load reached its maximum. Excessive damage was observed after reaching the peak load. At this stage, some longitudinal bars of the beams and reinforcement of the wall were exposed due to the spalling of cover concrete, and buckling of some of the wall and openings reinforcement at the first story were observed. The above mentioned cracking progress was common to all specimens. For specimen N1, at +0.5% drift angle, spalling of concrete at the boundary between wall panel and beam of the first story occurred; while, severe damage was observed at the base of the compression side column of the first story. At the drift angle of +0.75%, shear sliding occurred at the top of the first story wall panel, followed by sudden strength degradation. For specimen L1, the shear cracks in the wall of the first story and the flexural cracks in the tensile column of the first story were observed at a drift angle of +0.04%. At a drift angle of +0.25%, the cracks in the upper part of the opening progressed along the opening reinforcement. At drift angle of -0.5%, buckling of longitudinal reinforcement around the opening of the first story took place and severe damage of concrete was observed at -0.75 drift angle. At the drift angle of +1.5%, shear sliding occurred in the wall of the first story. The lateral reinforcing bars of the first story wall panel were bent severely, and cracks have propagated extensively along the wall reinforcements. The strength degradation after the peak load did not drop suddenly like observed for the case of specimen N1. As for specimen L3, the cracks in the wall of the first story and in the upper comer of the opening were observed at a drift angle of 0.05%and then the stiffness was decreased. Since a drift angle of 1.0%, the strength was gradually decreased without shear sliding observed in the wall of the first story. Moreover, damage to the boundary beam between walls was negligible till the end of the loading. For the central opening location and the difficulties of composing the compressive strut over two stories, the shear cracks over two stories were only a few.

3.2. Lateral load–drift angle relation

Figures 3(a) to 5(a) show the relationships between the lateral load and the drift angle. Table 5 summarizes the maximum lateral load and the corresponding drift angle. It can be seen that specimen N1 has the highest shear strength, and that the shear strength of L1 is lower than that of L3 because the opening location of L1 is eccentric. It can be also found, in both tests for specimens with openings, that the strengths attained during the positive direction loading are larger than those during negative direction loading. The strength degradation after the peak load can be seen more or less in both specimens. However, strength degradation is not sudden for L1 and L3. With respect to the failure mode, L1 failed in a comparatively ductile manner after flexural yielding of the short span beams and reached the final stage due to the shear slip damage of the wall.

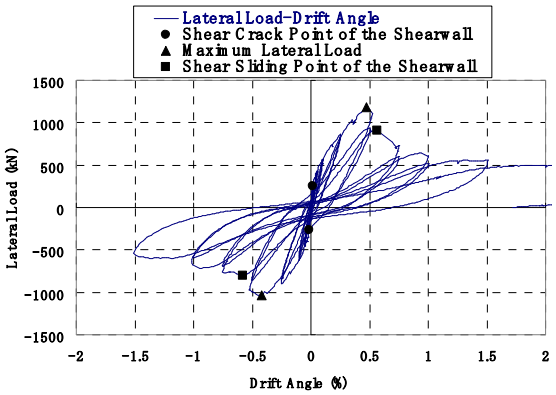

(a) (b)

Figure 3. (a) Hysteresis curve and (b) observed damage at the end of test - specimen N1-

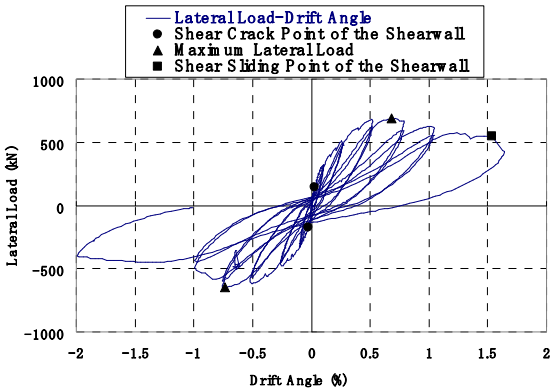

(a) (b)

Figure 4. (a) Hysteresis curve and (b) observed damage at the end of test - specimen L1-

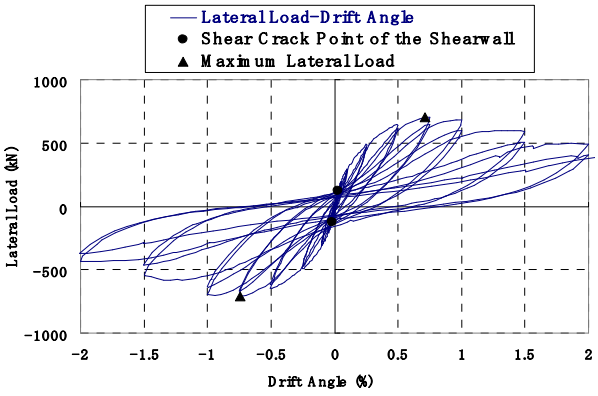

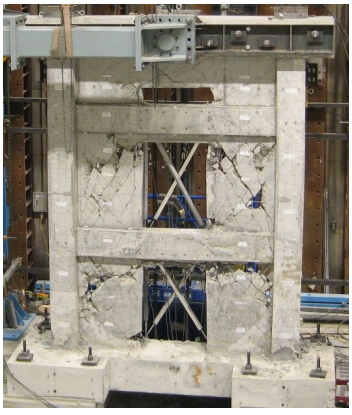

(a) (b)

Figure 5. (a) Hysteresis curve and (b) observed damage at the end of test - specimen L3-

Table 5. Maximum lateral loads and corresponding drift angles

	Positive direction		Negative direction	
	Maximum load (kN)	Drift angle (%)	Maximum load (kN)	Drift angle (%)
N1	1179	0.48	-1039	-0.42
L1	686	0.68	-649	-0.74
L3	701	0.71	713	-0.74

4. PREDICTION OF THE SHEAR STRENGTH

A simple method was used to estimate the shear strength, Q_{su}, of a structural wall with openings based on shear strength of a structural wall without openings which is given by:

$$Q_{su} = r_u.V_u \tag{2}$$

Where, r_u is the shear strength reduction factor and V_u is the shear strength of a structural wall without openings.

4.1. Shear strength reduction factor of AIJ standard

In the design practice of the Architectural Institute of Japan standard (AIJ, 2010), the strength reduction factor, r_u, adopted to calculate the shear strength of a structural wall with openings was defined as follow:

$$r_u = \min(r_1, r_2, r_3) \tag{3}$$

Where, $r_1 = 1 - 1.1 l_0 / l$, $r_2 = 1 - 1.1\sqrt{(h_0.l_0)/(h.l)}$ and $r_3 = 1 - 0.5(1 + l_0/l)h_0/h$. The maximum opening ratio is limited to 0.4 in the AIJ standard when the wall strength reduction factor due to openings is determined based on the shear strength of a structural wall without openings.

4.2. Ono's shear strength reduction factor

Considering the effective diagonal compression field of the concrete panel, as shown in Figure 6, strength reduction factor, r_u, was proposed by Ono (Ono and Tokuhiro, 1992; Ono, 1995) as follow:

$$r_u = \sqrt{\sum A_e / h.l} \tag{4}$$

Where, A_e is the area of the effective diagonal compression field, h is the distance between the upper and lower beams and l is the distance between the two boundary columns. Ono's strength reduction factor takes into account the opening location as well as opening dimensions. For multi-story wall with openings, Ono's reduction factor is taken as the minimum of Ono's reduction factor of each story.

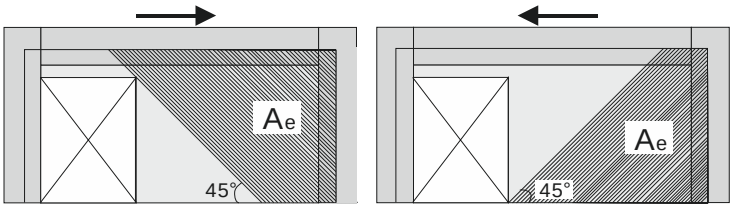

(a) Positive loading (b) Negative loading

Figure 6. Area of the wall panel forming a compression field

4.3. Shear strength of structural wall without openings

In this study, two methods were used to estimate the shear strength, V_u, of a structural wall without openings. The first method is based on truss and arch mechanism given by (AIJ, 2004):

$$V_u = t_w l_{wb} p_s \sigma_{sy} \cot\phi + \tan\theta(1-\beta) t_w l_{wa} \nu \sigma_B / 2 \tag{5}$$

with,

$$\tan\theta = \sqrt{[(h_w/l_{wa})^2 - 1]} - h_w/l_{wa} \quad (6)$$

$$\beta = \left(1 - \cot^2\phi\right) p_s \sigma_{sy} / \left(\nu \sigma_B\right) \quad (7)$$

Where, t_w is the thickness of the wall panel, h_w is the height of the wall, l_{wb} and l_{wa} are the equivalent lengths of the wall panel in the truss mechanism and arch mechanism, respectively, σ_B is the compressive strength of concrete, σ_{sy} is the yield strength of the shear reinforcement within the wall panel, p_s is the shear reinforcement ratio within the wall panel, ϕ is the angle of the compressive strut in the truss mechanism and ν is the effectiveness factor for the compressive strength of concrete.

The second method is based on Arakawa's equation given by (JBDPA, 2001):

$$V_u = \left[\frac{0.053 p_{te}^{0.23} (17.6 + F_c)}{M/(Q.l) + 0.12} + 0.845\sqrt{p_{se}.\sigma_{wy}} + 0.1\sigma_{0e} \right] .b_e.j_e \quad (8)$$

Where, p_{te} is the equivalent tensile reinforcement ratio, F_c is the concrete compressive strength, (M/Ql) is the shear span ratio, p_{se} is the transversal equivalence ratio, σ_{wy} is the yield strength of the transversal reinforcement, σ_{0e} is the axial stress, b_e is the equivalent wall thickness and j_e is the stress center distance.

4.4. Results of the shear strength prediction

Comparison of the calculated shear strengths using the mentioned methods given by Eq.(5) and Eq.(8) to the experimental results is summarized in Table 6 and Table 7, respectively. In these two tables, Q_{Exp}, Q_{AIJ}, Q_{Ono} are the shear strength obtained from the test, using the AIJ standard reduction factor and the Ono's reduction factor, respectively. Arakawa's equation gives conservative values of shear strength because the formula is based on lower limit of shear strength. Shear strength prediction based on truss and arch mechanism agreed well with the experimental values of shear strength. Using truss and arch mechanism equation, shear strength calculated using AIJ's reduction factor agree well with the experimental results in negative direction. While in the positive direction, the shear strength is underestimated. This difference is due to the fact that AIJ's reduction factor is the same in the positive and negative loading direction and does not reflect the opening position. Ono's reduction factor method gave a better estimation of the shear strength either in positive and negative loading direction, because the effective area of wall corresponding to the compressive field in positive direction and negative direction was taken into account.

Table 6. Comparison of the shear strengths using Eq. 5

	Positive direction			Negative direction		
	Q_{Exp} (kN)	Q_{AIJ} (kN)	Q_{Ono} (kN)	Q_{Exp} (kN)	Q_{AIJ} (kN)	Q_{Ono} (kN)
N1	1179	1120		-1039	-1120	
L1	686	582	784	-649	-582	-717
L3	701	619	638	-713	-619	-638

Table 7. Comparison of the shear strengths using Eq. 8

	Positive direction			Negative direction		
	Q_{Exp} (kN)	Q_{AIJ} (kN)	Q_{Ono} (kN)	Q_{Exp} (kN)	Q_{AIJ} (kN)	Q_{Ono} (kN)
N1	1179	854		-1039	-854	
L1	686	461	598	-649	-461	-547
L3	701	463	487	-713	-463	-487

5. NONLINEAR FEM ANALYSIS

5.1. Analytical model

A two-dimensional static nonlinear FEM analysis was carried out for the tested specimens. The validity of analytical model is examined to investigate the stress transfer mechanism of RC shear wall with openings. The finite element mesh for specimen L1 is shown in Figure 7. The element size of the mesh in the wall panels was 50x50mm. Each node at the bottom of the foundation beam had pin support to restrain vertical and lateral displacement. Loading beam and foundation beam were assumed to be elastic. Horizontal and vertical reinforcement was smeared assuming a perfect bond but diagonal reinforcement was neglected. The FEM non-linear analysis software FINAL was used in this analysis.

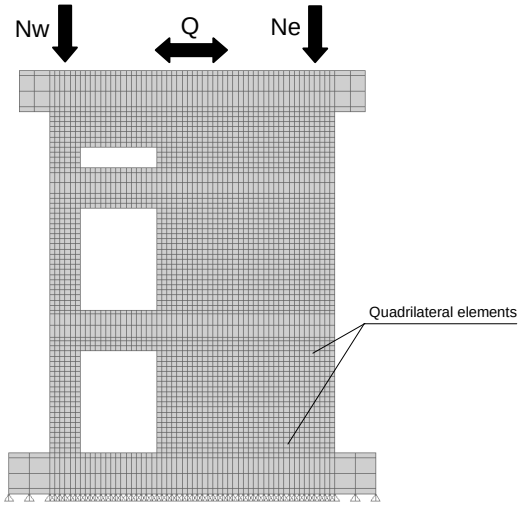

Figure 7. Finite element mesh (specimen L1)

5.2. Element Model

Mechanical properties of material model used in the analysis are thus given in Table 3 and Table 4. Quadrilateral plane stress elements were used for concrete. Reinforcing bars were substituted equivalent layers with stiffness in the bar direction and superposed on the quadrilateral elements assuming a perfect bond. For Reinforcing bars material, The von Mises yield surface is employed to judge yielding under a multi-axial stress field along with the associated flow rule for isotropic hardening. The stress-strain relationship under stress reversal follows Ciampi's model (Ciampi *et al.*, 1982). As for the stress-strain relationship of concrete, a modified Ahmad model was adopted for the compressive stress-strain curve (Ahmad and Shah, 1982). The model by Kupfer and Gerstle (1973) was adopted as the fracture criterion of concrete under biaxial stress state, and the compressive strength reduction factor was adopted from Naganuma (Naganuma, 1991). The concrete tension stiffing model and the shear transfer model after cracks proposed by Naganuma was adopted (Naganuma and Ohkubo, 2000).

5.3. Analysis results

Analytical lateral load-drift angle relations are compared with the experimental results in Figure 8. Table 8 shows a comparison between the experimental and the FEM peak loads with the corresponding drift angle. The analytical envelop curves matched well with the experimental results for all specimens as illustrated in Fig. 12. The FEM peak loads agreed well with the experimental ones. As for the corresponding drift angles, a good agreement is observed for specimens N1 , while for specimens L1 and L1, with larger opening ratio, the model underestimate this value. This can be explained by the fact that, for specimens with large openings, the flexural component became more important than in the case of specimen without openings.

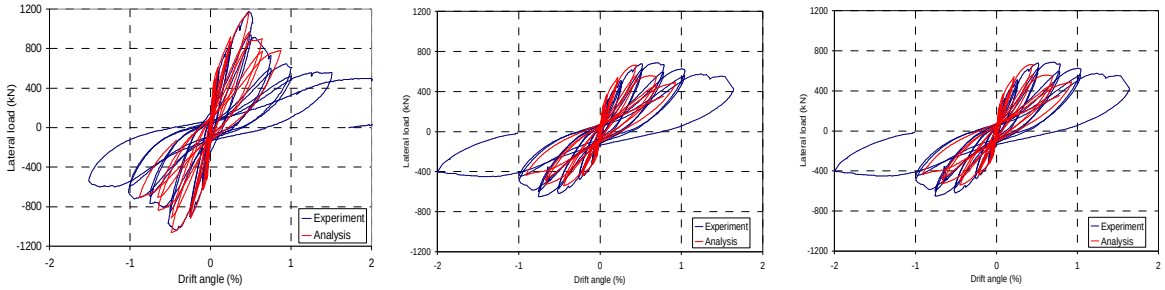

(a) (b) (c)

Figure 8. Lateral load–drift angle relationships for (a) N1, (b) L1 and (c) L3

Table 8. Comparison of the maximum lateral loads

	Positive direction					Negative direction				
	Maximum load (kN)			Drift angle (%)		Maximum load (kN)			Drift angle (%)	
	Q_{Exp}	Q_{FEM}	Q_{Exp}/Q_{FEM}	R_{Exp}	R_{FEM}	Q_{Exp}	Q_{FEM}	Q_{Exp}/Q_{FEM}	R_{Exp}	R_{FEM}
N1	1179	1183	1.00	0.48	0.44	-1039	-1183	0.88	-0.42	-0.44
L1	686	649	1.06	0.68	0.38	-649	-573	1.13	-0.74	-0.46
L3	701	615	1.14	0.71	0.44	-713	-610	1.17	-0.74	-0.44

6. CONCLUSIONS

Cyclic loading tests were conducted on three 40%-scale specimens in order to evaluate the shear behaviour of RC structural walls with and without openings. The specimens represented the lower three stories of a six-story reinforced concrete building. The following conclusions can be drawn.

Shear strength of a structural wall was different between positive and negative loading directions due to the opening location and the damage state. For L1 specimen, shear strength obtained while loading from the opening side was larger than that obtained from the opposite side. The raison was due to the existence of eccentric openings that affected the formation of concrete strut. Shear transfer mechanism was interrupted and the concrete damage at the corner of the opening caused the sliding failure of wall. It is recommended that this phenomenon should be assessed carefully through other tests and should be taken into account in the future design standard.

Since Ono's reduction factor method considered the effective concrete compressive field of the structural wall, the calculated shear strengths using this method agreed well with the experimental ones and at the same time confirmed the shear transfer mechanism. It is worth to mention that, damage to the compressed concrete of the first story wall, was the principal factor which influenced the shear capacity of the multi-story structural walls.

In order to simulate the behavior of the specimens, a cyclic nonlinear finite elements analysis was carried out using a two-dimensional model. The analysis gave a good agreement for the maximum peak loads.

ACKNOWLEDGEMENTS

The reported research herein was supported by the grants from the Grants-in-Aid for Scientific Research of Japan (No. 16206056), which is gratefully acknowledged. The authors would like also to thank the graduate students M. Warashina, K. Mori, M. Doi and K. Chosa for their great assistance and help during the experiments and the data process.

REFERENCES

Ahmad, S. H. and Shah, S. P. (1982), Complete triaxial stress-strain curve for concrete, *ASCE J. Struct. Div.*, 108(ST4), pp. 728-742.

Architectural Institute of Japan (2010), *AIJ Standard for Structural Calculation of reinforced Concrete Structures (Revised 2010)*, Architectural Institute of Japan, Tokyo, Japan. (in Japanese)

Architectural Institute of Japan (2004), *Guidelines for Performance Evaluation of Earthquake Resistant Reinforced Concrete Buildings*, Architectural Institute of Japan, Tokyo, Japan.

Architectural Institute of Japan (1998), *Report on the Hanshin-Awaji Earthquake Disaster Building Series Volume 1: Structural Damage to Reinforced Concrete Building*, Architecture Institute of Japan, Tokyo, Japan.

Balkaya, C., and Kalkan, E. (2004), Three-Dimensional Effects on Openings of Laterally Loaded Pierced Shear Walls, *ASCE J. Struct. Eng.*, 130:10, pp 1506-15414.

Bechtoula, H., and Ousalem, H. (2005), The 21 May 2003 Zemmouri (Algeria) Earthquake: Damages and Disaster Responses, *J. Adv. Concr. Techno.*, 3(1) 161-174.

Brun, M., Labbe, P., Bertrand, D. and Courtois A. (2011), Pseudo-dynamic tests on low-rise shear walls and simplified model based on the structural frequency drift, *Eng. Struct.*, 33(3):796-812.

Ciampi, V., Eligehausen, R., Bertero, V.V. and Popov, E.P. (1982), *Analytical model for concrete anchorages of reinforcing bars under generalized excitations*, Report No. UCB/EERC 82-23, Earthquake Engineering Research Center, University of California, Berkeley, California.

FINAL/99, Finite elements analysis program for the nonlinear behaviour of concrete structures, ITOCHU Techno-Solutions Corporation.

Guan, H., Cooper, C. and Lee D.J. (2010), Ultimate strength analysis of normal and high strength concrete wall panels with varying opening configurations, *Eng. Struct.*, 32(5):1341–1355.

Japan Building Disaster Prevention Association (2001), Standard for Seismic Evaluation of Existing Reinforced Concrete Buildings, Japan Building Disaster Prevention Association, Tokyo, Japan

Kabeyasawa, T., Kabeyasawa, T., Kim Y., Kabeyasawa, T. and Bae, K. (2009), Tests on Reinforced Concrete Columns with Wing Walls for Hyper-Earthquake Resistant System, 3rd International Conference on Advances in Experimental Structural Engineering, San Francisco, USA.

Kim, H. S. and Lee, D.G. (2003), Analysis of shear wall with openings using super elements, *Eng. Struct.*, 25(8): 981–991.

Kupfer, H. B. and Gerstle, K.H. (1973), Behavior of Concrete under Biaxial Stress, *ASCE J. Eng. Mech. Div.*, 99(EM4), pp. 853-866.

Lopes, M.S. (2001), Experimental shear-dominated response of RC walls. Part II: Discussion of results and design implications, *Eng. Struct.*, 23(5): 564–574.

Maekawa, K., Pimanmas, A. and Okamura, H. (2003), *Nonlinear Mechanics of Reinforced Concrete*, Spon Press, London.

Naganuma, K. (1991), Nonlinear Analytical Model for Reinforced Concrete Panels under In-Plane Stresses, *J. Struct. Constr. Eng.*, No.421, pp. 39-48.

Naganuma, K. and Ohkubo, M. (2000), An Analytical Model For Reinforced Concrete Panels under Cyclic Stresses. *J. Struct. Constr. Eng.*, No.536, pp. 135-142.

Ono, M. (1995). Experimental Study on Reinforced Concrete Opening Wall above Opening Periphery Ratio 0.4, Part1~Part2, *Summaries of Technical Papers of Annual Meeting of Architectural Institute of Japan* C-2, Structures IV: 147–150. (in Japanese)

Ono, M. and Tokuhiro, I. (1992), A Proposal of Reducing Rate for Strength due to Opening Effect of Reinforced Concrete Framed Shear Walls, *J. Struct. Constr. Eng.*, No.435, pp. 119-129.

Thomson, E.D., Perdomo, M.E., Picón, R., Marante, M.E. and Flórez-López, J. (2009), Simplified model for damage in squat RC shear walls, *Eng. Struct.*, 31(10):2215-2223.